Diabetologia (2016) 59:1276–1286
DOI 10.1007/s00125-016-3912-9

ARTICLE

Bavachinin, as a novel natural pan-PPAR agonist, exhibits unique synergistic effects with synthetic PPAR-γ and PPAR-α agonists on carbohydrate and lipid metabolism in *db*/*db* and diet-induced obese mice

Li Feng[1,2] · Huan Luo[3] · Zhijian Xu[4] · Zhuo Yang[4] · Guoxin Du[1] · Yu Zhang[2] · Lijing Yu[2] · Kaifeng Hu[3] · Weiliang Zhu[4] · Qingchun Tong[5] · Kaixian Chen[1,4] · Fujiang Guo[1] · Cheng Huang[2] · Yiming Li[1]

Received: 12 September 2015 / Accepted: 10 February 2016 / Published online: 16 March 2016

Abstract

Aims/hypothesis Pan-peroxisome proliferator-activated receptor (PPAR) agonists have long been sought as therapeutics against the metabolic syndrome, but current PPAR agonists show limited efficacy and adverse effects. Natural herbs provide a structurally untapped resource to prevent and treat complicated metabolic syndrome.

Methods Natural PPAR agonists were screened using reporter gene, competitive binding and 3T3-L1 pre-adipocyte differentiation assays in vitro. The effects on metabolic phenotypes were verified in *db*/*db* and diet-induced obese mice. In addition, potentially synergistic actions of bavachinin (BVC, a novel natural pan-PPAR agonist from the fruit of the traditional Chinese glucose-lowering herb malaytea scurfpea) and synthetic PPAR agonists were studied through nuclear magnetic resonance, molecular docking, reporter gene assays and mouse studies.

Results BVC exhibited glucose-lowering properties without inducing weight gain and hepatotoxicity. Importantly, BVC synergised with thiazolidinediones, which are synthetic PPAR-γ agonists, and fibrates, which are PPAR-α agonists, to induce PPAR transcriptional activity, as well as to lower glucose and triacylglycerol levels in *db*/*db* mice. We further found that BVC occupies a novel alternative binding site in addition to the canonical site of synthetic agonists of PPAR, and that the synthetic PPAR-γ agonist rosiglitazone can block BVC binding to this canonical site but not to the alternative site.

Conclusions/interpretation This is the first report of a synergistic glucose- and lipid-lowering effect of BVC and synthetic agonists induced by unique binding with PPAR-γ or -α. This combination may improve the efficacy and decrease the toxicity of marketed drugs for use as adjunctive therapy to treat the metabolic syndrome.

Electronic supplementary material The online version of this article (doi:10.1007/s00125-016-3912-9) contains peer-reviewed but unedited supplementary material, which is available to authorised users.

✉ Fujiang Guo
gfj@shutcm.edu.cn

✉ Cheng Huang
chuang@shutcm.edu.cn

✉ Yiming Li
ymli@shutcm.edu.cn

[1] Department of TCM Chemistry, School of Pharmacy, Shanghai University of Traditional Chinese Medicine, 1200 Cailun Road, Shanghai 201203, People's Republic of China

[2] Laboratory of Drug Discovery, School of Pharmacy, Shanghai University of Traditional Chinese Medicine, 1200 Cailun Road, Shanghai 201203, People's Republic of China

[3] State Key Laboratory of Phytochemistry and Plant Resources in West China, Kunming Institute of Botany, Chinese Academy of Sciences, Kunming, People's Republic of China

[4] CAS Key Laboratory for Membrane Research, Drug Discovery and Design Center, Shanghai Institute of Materia Medica, Chinese Academy of Sciences, Shanghai, People's Republic of China

[5] The Brown Foundation Institute of Molecular Medicine, University of Texas Health Science Center at Houston, Houston, TX, USA

Keywords Alternative binding site · Bavachinin · Canonical ligand-binding pocket · Carbohydrate metabolism · Lipid metabolism · Pan-PPAR agonist · Synergistic effects

Abbreviations

ABS	Alternative binding site
ALT	Alanine transaminase
AST	Aspartate transaminase
BVC	Bavachinin
CLBP	Canonical ligand-binding pocket
DIO	Diet-induced obese
EC_{50}	Half maximal effective concentration
HDL-/LDL-C	HDL-/LDL-cholesterol
HFD	High-fat diet
ipGTT	Intraperitoneal glucose tolerance test
ipITT	Intraperitoneal insulin tolerance test
LBD	Ligand-binding domain
LXR	Liver x receptor
PGC1α	Peroxisome proliferative activated receptor, γ, coactivator 1 α
PPAR	Peroxisome proliferator-activated receptor
PGZ	Pioglitazone
RSG	Rosiglitazone
TCH	Total cholesterol
TG	Triacylglycerol
TRAP220	Mediator complex subunit 1
TR-FRET	Time-resolved fluorescence resonance energy transfer
TZD	Thiazolidinedione

Introduction

The metabolic syndrome is a cluster of metabolic abnormalities, including type 2 diabetes, obesity, dyslipidaemia, insulin resistance, liver steatosis and hypertension [1]. Peroxisome proliferator-activated receptors (PPARs) belong to the nuclear receptor superfamily that function as ligand-inducible transcription factors and control the expression of multiple target genes [2, 3]. Pharmacological activation of each of three PPAR isoforms (α, β/δ and γ) is effective at correcting a specific aspect of the metabolic syndrome, such as insulin resistance, dyslipidaemia and hyperglycaemia [2]. Fibrates such as bezafibrate and fenofibrate, which are synthetic PPAR-α agonists, have been used to treat dyslipidaemia by lowering triacylglycerol (TG) levels and increasing HDL-cholesterol (HDL-C) levels [4]. Thiazolidinediones (TZDs), such as rosiglitazone (RSG) and pioglitazone (PGZ), which are classic selective PPAR-γ agonists, are used as insulin sensitisers to treat type 2 diabetes [5–8]. Recent studies have highlighted the metabolic functions of PPAR-β/δ activators in the treatment of obesity [9–14]. Thus, the activation of three PPAR subtypes simultaneously (pan-PPAR agonism) is a promising avenue for reversal of multiple metabolic syndrome disorders.

Evidence has suggested that pan-PPAR agonists could complement each other and circumvent the limitations of selective or dual PPAR agonism. However, there are still some limitations to developing pan-PPAR agonists. Bezafibrate, a PPAR-α agonist, has been found to activate all three PPAR isoforms [15, 16], but its glucose-lowering effect is not significant in clinical studies [17]. Most pan-PPAR agonists, including GW677954, DRL-11605, PLX-204, GW625019 and netoglitazone, have been discontinued because of safety problems [18–20]. Additionally, preclinical studies on pan-PPAR agonists LY465608 and BPR1H036 are not progressing smoothly [21–24].

Natural products have served as the source and inspiration for a large number of current drugs. Malaytea scurfpea fruit, the seed of *Psoralea corylifolia* Linn., has been used in traditional Chinese formulas to prevent and treat type 2 diabetes in clinical practice [25, 26]. In this study, bavachinin (BVC), a component of malaytea scurfpea fruit, is identified as a novel natural pan-PPAR agonist in vitro and in vivo. Interestingly, BVC does not antagonise, but synergises with TZDs and fibrates in metabolic syndrome phenotypes. This synergism is induced by unique binding modes of BVC with PPAR-γ or -α.

Methods

All experimental details are shown in the electronic supplementary material (ESM) Methods.

Isolation and purification of BVC See ESM Methods for details.

Reporter gene assay 293T cells were transfected over a 6 h period with target expression plasmid, relevant reporter plasmid, pREP7 reporter and FuGENE-HD transfection reagent, and were subsequently treated with compounds for 24 h. Luciferase activity was detected using the Dual-Luciferase Reporter Assay System (Promega, Madison, WI, USA).

TR-FRET assay LanthaScreen time-resolved fluorescence resonance energy transfer (TR-FRET) competitive binding or coactivator assays (Invitrogen, Carlsbad, CA, USA) use the ligand-binding domain (LBD) of human nuclear receptors tagged with glutathione *S*-transferase (GST), the terbium-labelled anti-GST antibody and the fluorescent small molecule or coactivator peptide.

3T3-L1 differentiation 3T3-L1 cells were purchased from Cell Bank of Shanghai Institutes of Biological Sciences, Chinese Academy of Sciences, China. The cells were induced and maintained in the presence of test compounds (day 0–day 6), and then stained with Oil Red O as previously reported [27]. To investigate the effects on the expression of PPAR target genes, 3T3-L1 cells exposed to compounds were harvested on days 0, 2 or 6.

Animal experiments In accordance with the Guide for the Care and Use of Laboratory Animals, all animal studies were guided by the Animal Ethics Committee of Shanghai University of Traditional Chinese Medicine.

Thirty-three 9-week-old female *db*/*db* mice were randomly administered with vehicle, or 4 mg kg^{-1} day^{-1} RSG or 100 mg kg^{-1} day^{-1} BVC by gavage for 3 weeks ($n = 11$). Twenty-one 19-week-old female diet-induced obese (DIO) mice received RSG (100 mg/kg) or BVC (2 g/kg) milled in a high-fat diet (HFD) or regular HFD (Research Diets, New Brunswick, NJ, USA) for 3 weeks ($n = 7$). The age-matched, lean wild-type C57BL/6J mice were treated as normal control groups ($n = 10$).

To study the synergistic effects on glucose metabolism, 53 male *db*/*db* mice were randomly administered with vehicle, 2 mg kg^{-1} day^{-1} or 4 mg kg^{-1} day^{-1} RSG, 50 mg kg^{-1} day^{-1} or 100 mg kg^{-1} day^{-1} BVC, or 2 mg kg^{-1} day^{-1} RSG plus 50 mg kg^{-1} day^{-1} BVC by gavage for 4 weeks ($n = 8$–9). To study the synergistic effects on lipid regulation, groups of *db*/*db* mice were treated with one of the following by gavage for 4 weeks: (1) vehicle; (2) fenofibrate, 25 mg kg^{-1} day^{-1} or 100 mg kg^{-1} day^{-1}; (3) BVC, 50 mg kg^{-1} day^{-1} or 100 mg kg^{-1} day^{-1}; or (4) fenofibrate, 25 mg kg^{-1} day^{-1}, plus BVC, 50 mg kg^{-1} day^{-1}.

At the end of treatment, all overnight-fasted mice were anaesthetised. Blood samples were collected by cardiac puncture, and multiple organs and tissues were harvested and either fixed in formalin or snap frozen and stored at −80°C.

Metabolic studies All mice were subjected to an overnight (8–12 h) fast followed by intraperitoneal glucose tolerance test (ipGTT) and non-fasting conditions followed by intraperitoneal insulin tolerance test (ipITT). Hepatic lipids were extracted as described previously [27], and TGs and total cholesterol (TCH) were detected using colorimetric kits. Values were calculated as nmol/l (TG and TCH) per mg wet tissue. Serum levels of insulin, adiponectin, leptin, NEFA, TG, TCH, HDL-C, LDL-cholesterol (LDL-C), alanine transaminase (ALT) and aspartate transaminase (AST) were analysed from collected fasted blood using commercial kits.

Histochemistry Livers were fixed, processed and stained with haematoxylin and eosin (H&E) and Oil Red O as described [27].

Mouse cDNA genome-wide gene expression analysis The details are shown in ESM Methods.

Quantitative real-time PCR Total RNA was prepared using TRIzol reagent (TaKaRa, Dalian, China). The first strand cDNA was synthesised using a reverse transcription kit (Thermo, Waltham, MA, USA), and was amplified with SYBR Green QPCR Master Mix (Applied Biosystems, Waltham, MA, USA) using an ABI StepOnePlus sequence detector (Applied Biosystems).

Nuclear magnetic resonance All ^{19}F nuclear magnetic resonance (NMR) experiments were performed at 298 K on a Bruker 500 MHz AVANCE spectrometer equipped with 5 mm QCI-F cryoprobe without ^{1}H decoupling, using standard pulse sequence 'zg' provided with Topspin 3.0.

Molecular docking The crystal structure of PPAR-γ (PDB code 3K8S) was retrieved from the Research Collaboratory for Structural Bioinformatics (RCSB) protein data bank. Docking was performed using Glide 5.6 (Schrödinger, New York, NY, USA) with its SP mode.

Statistical analysis All data are expressed as mean ± SEM. Statistical analysis was performed using SPSS 16.0 (SPSS, Chicago, IL, USA). Between-group differences were determined by one-way ANOVA with the least significant difference (LSD) test. All statistical tests are two-tailed. A value of $p \leq 0.05$ was considered to be statistically significant. The IC_{50} and half maximal effective concentration (EC_{50}) values were calculated using GraphPad Prism 5.0 (GraphPad Software, La Jolla, CA, USA). Experimenters were not blind to group assignment and outcome assessment, and no data were excluded from the experimental results.

Results

BVC is a natural pan-PPAR agonist with potent binding affinities A reporter gene assay was used to determine the activities of BVC on PPAR-α, -β/δ or -γ. As shown in Fig. 1, BVC (Fig. 1a) dose-dependently induced the transcriptional activities of the mouse LBD (Fig. 1b–d) and full lengths (Fig. 1e–g) of the three PPAR isoforms. Notably, BVC showed stronger activities with PPAR-γ than with PPAR-α and PPAR-β/δ ($EC_{50} = 0.74$ μmol/l, 4.00 μmol/l and 8.07 μmol/l, respectively; Table 1).

To examine the cellular effect of BVC on PPAR-γ, insulin, dexamethasone and RSG or BVC were used to induce differentiation of 3T3-L1 pre-adipocytes. BVC promoted 3T3-L1 adipocyte differentiation in a dose-dependent manner (Fig. 1h). 3T3-L1 differentiation was effectively activated by

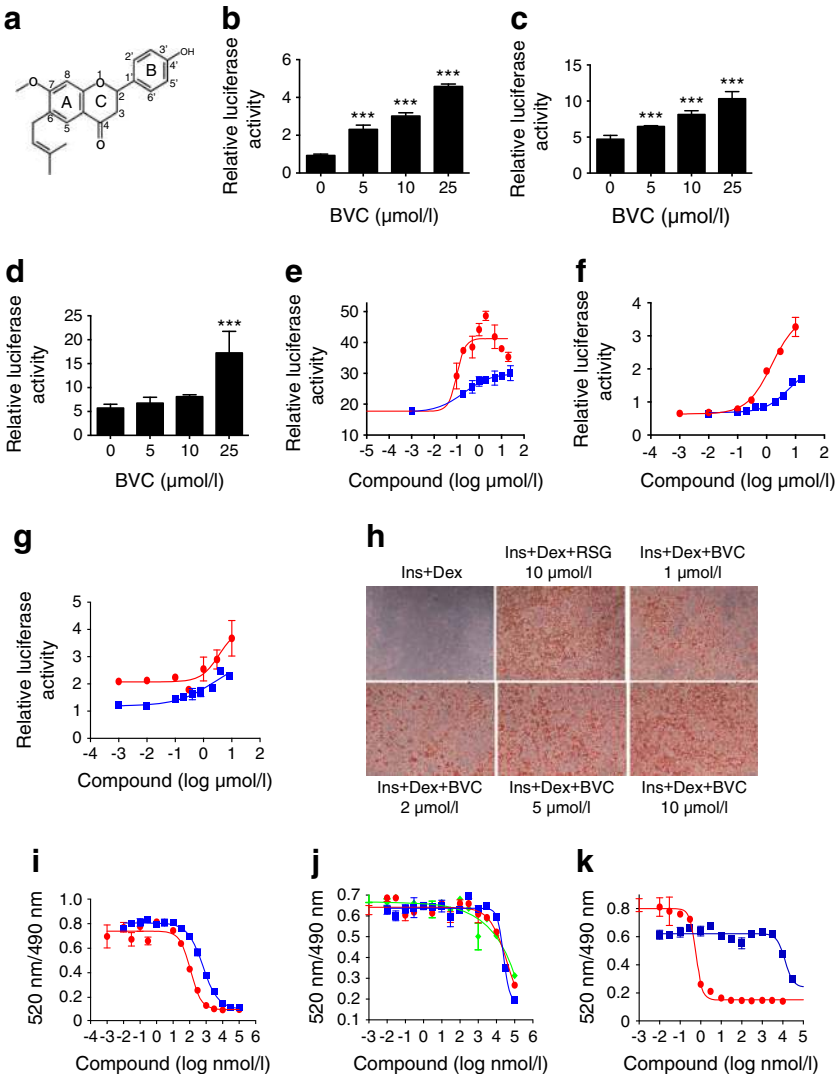

Fig. 1 BVC functions as a potent pan-PPAR agonist. (**a**) Structure of BVC. (**b**–**d**) BVC induced the transcriptional activities of LBDs of mouse PPAR-γ (**b**), -α (**c**) and -β/δ (**d**). ***$p < 0.001$ vs 0 μmol/l BVC. (**e**–**g**) Compounds induced the transcriptional activity of full-length mouse PPAR-γ (**e**), -α (**f**) and -β/δ (**g**). Blue, BVC; Red, RSG (**e**), WY14643 (**f**) and GW0742 (**g**). (**h**) BVC-induced 3T3-L1 pre-adipocyte differentiation. Cells were exposed to BVC or RSG at the beginning of pre-adipocyte induction (day 0). The adipocytes were stained with Oil Red O on day 6. Ins+Dex, 10 μg/ml insulin + 1 μmol/l dexamethasone. (**i**–**k**) Binding to LBDs of human PPAR-γ (**i**), -α (**j**) and -β/δ (**k**) in a TR-FRET competitive binding assay. Blue, BVC; red, RSG (**i**), WY14643 (**j**) and GW0742 (**k**); green, fenofibric acid (**j**)

1 μmol/l BVC, and almost fully by 10 μmol/l BVC. The results suggest that BVC activates PPAR-γ at a cellular level.

Competitive binding assays (Fig. 1i–k) showed that BVC had stronger binding to human PPAR-γ (K_i = 223 nmol/l; Table 1) than to human PPAR-α and -β/δ (K_i = 7.88 and 5.28 μmol/l; Table 1). Moreover, BVC has a fivefold weaker binding affinity than RSG for PPAR-γ, and has twofold stronger binding affinity than fenofibric acid and WY14643 for PPAR-α.

In contrast to the full PPAR-γ agonist RSG and PPAR-α agonist GW7647, BVC did not induce the recruitment of

Table 1 Binding affinity constants, inhibitory concentrations and effective concentrations of tested compounds for three PPAR subtypes

Compound	PPAR-α			PPAR-β/δ			PPAR-γ		
	K_i	IC_{50}	EC_{50}	K_i	IC_{50}	EC_{50}	K_i	IC_{50}	EC_{50}
BVC	7.881	21.043	4.001	5.275	12.819	8.072	0.223	0.622	0.738
RSG	ND	ND	ND	ND	ND	ND	0.041	0.113	0.129
GW7647	0.002	0.004	ND	ND	ND	ND	ND	ND	ND
WY14643	15.717	41.967	2.942	ND	ND	ND	ND	ND	ND
Fenofibric acid	17.216	45.969	ND	ND	ND	ND	ND	ND	ND
GW0742	ND	ND	ND	0.0003	0.0006	2.929	ND	ND	ND

Affinity constant (K_i, μmol/l), inhibitory concentration (IC_{50}, μmol/l), effective concentration (EC_{50}, μmol/l)

K_i and IC_{50} values were obtained from a human PPAR competitive binding assay; EC_{50} values were detected by using a mouse PPAR reporter gene assay. ND, not determined

classic transcriptional cofactors, peroxisome proliferative activated receptor, gamma, coactivator 1 α (PGC1α) and mediator complex subunit 1 (TRAP220/DRIP) (ESM Fig. 1a–c). Using reporter gene and coactivator recruitment assays, BVC did not activate other nuclear receptors related to the metabolic syndrome, such as liver x receptor (LXR)-α, LXR-β/δ and farnesoid x receptor (FXR) (ESM Fig. 1d–g), suggesting the specificity of BVC for PPARs.

BVC treatment ameliorates diabetes and hyperlipidaemia in *db*/*db* and DIO mice Next, we evaluated the glucose-lowering effects of BVC in leptin-receptor-deficient *db*/*db* mice and DIO mice. In groups of *db*/*db* mice with similar food intake (Fig. 2a), RSG greatly increased body weight by approximately 8 g within 3 weeks ($p<0.001$), whereas BVC treatment did not significantly induce weight gain (Fig. 2b). BVC treatment significantly decreased fasting and non-fasting glucose levels (Fig. 2c, d) and enhanced glucose tolerance (17% decrease in glucose AUC vs vehicle) and insulin sensitivity (34% decrease in glucose AUC vs vehicle) during intraperitoneal glucose tolerance test (ipGTT and ipITT in *db*/*db* mice (Fig. 2e, f). Similar results were detected in DIO mice (ESM Fig. 2). Insulin resistance, one hallmark of type 2 diabetes, is usually accompanied by hyperinsulinaemia. In both models, insulin levels were notably reduced by BVC comparable with the effect of RSG (Fig. 2g). Additionally, BVC significantly upregulated levels of adiponectin (Fig. 2h), which also promotes insulin sensitivity and decreases glucose

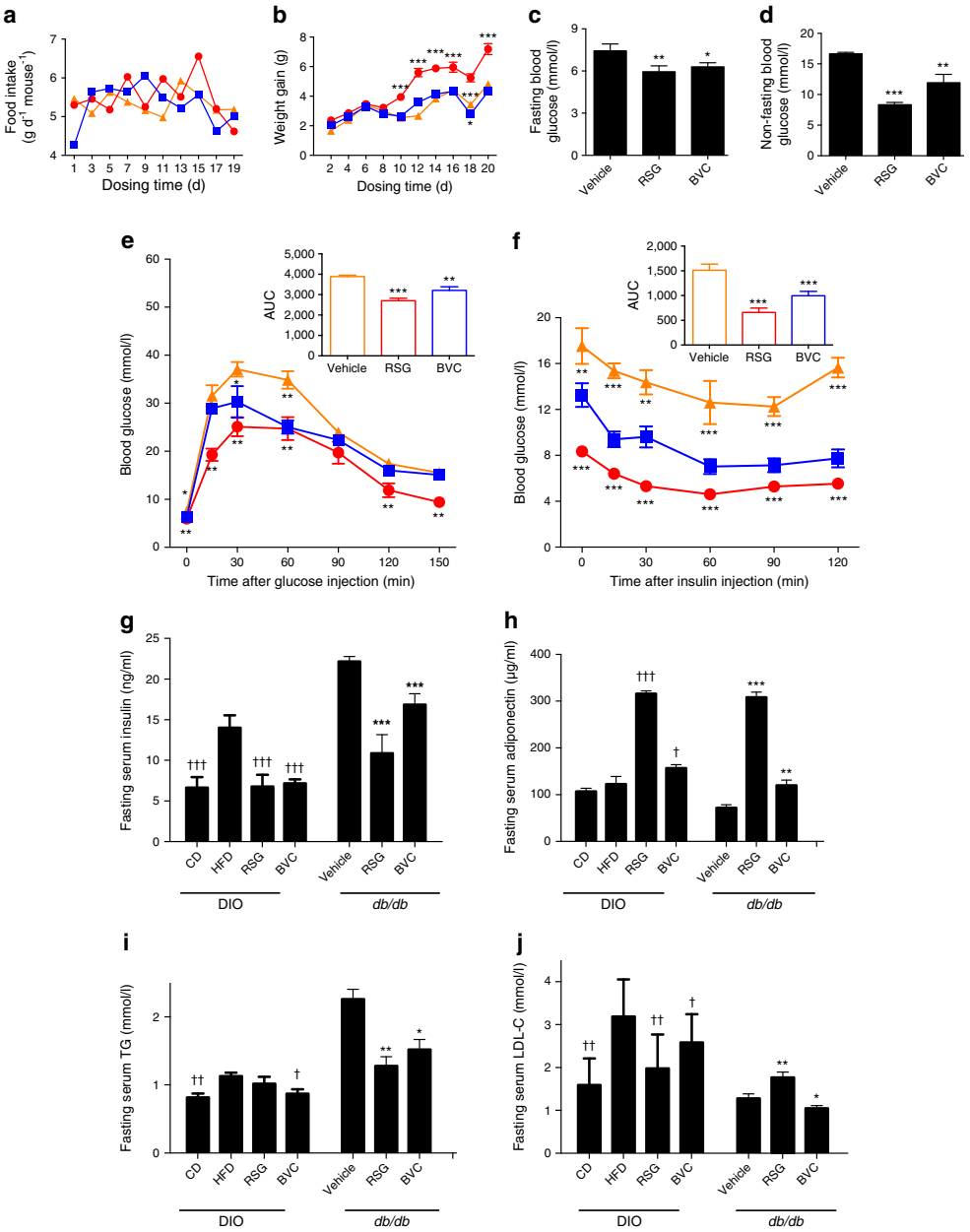

Fig. 2 BVC exhibits potent glucose-lowering effects in *db*/*db* mice. Mice were treated with vehicle or 100 mg kg^{-1} day^{-1} BVC or 4 mg kg^{-1} day^{-1} RSG for 3 weeks ($n=11$). (**a**) Food intake. (**b**) Weight gain. (**c**) Fasting blood glucose. (**d**) Non-fasting blood glucose. (**e**) Glucose levels during ipGTT (inset, AUC, mmol/l × min) were measured after an 8 h fast. (**f**) Glucose concentrations during ipITT (inset, AUC, mmol/l × min) were determined in non-fasting conditions. (**g**) Fasting serum insulin, (**h**) adiponectin, (**i**) TG and (**j**) LDL-C levels were investigated in DIO and *db*/*db* mice after an 8 h fast. Orange, vehicle; red, RSG; blue, BVC. $^{*}p<0.05$, $^{**}p<0.01$ and $^{***}p<0.001$ vs *db*/*db* vehicle mice. $^{\dagger}p<0.05$, $^{\dagger\dagger}p<0.01$ and $^{\dagger\dagger\dagger}p<0.001$ vs DIO HFD mice. CD, chow diet; d, day

production in the liver [28]. Meanwhile, BVC, but not RSG, decreased serum leptin levels to further alleviate insulin resistance in DIO mice (ESM Fig. 2f). The above results demonstrated that BVC ameliorates insulin resistance and glucose metabolism in *db*/*db* and DIO mice.

High serum TG and LDL-C and low HDL-C levels are characterised as major lipid risk factors for patients with the metabolic syndrome [29]. In both mouse models, BVC lowered TG levels ($p < 0.05$), while RSG did not show consistent TG-lowering effects (Fig. 2i). Additionally, BVC reduced LDL-C levels in both models, while RSG increased LDL-C levels in *db*/*db* mice and decreased levels in DIO mice (Fig. 2j). Moreover, BVC strongly lowered serum NEFA in *db*/*db* mice and increased the levels of HDL-C/LDL-C in both models (ESM Fig. 3). The results indicate that BVC is more effective in dyslipidaemia than RSG in DIO.

BVC improves hepatotoxicity in *db*/*db* and DIO mice Non-alcoholic fatty liver, an additional feature of the metabolic syndrome [30], was observed in *db*/*db* and DIO mice (Fig. 3 and ESM Fig. 4). Oil Red O staining showed that BVC decreased lipid accumulation in liver compared with vehicle or RSG treatment (Fig. 3a), which was verified with hepatic lipid content quantification (Fig. 3b). Compared with RSG, BVC lowered liver TG content by approximately 50% and liver TCH contents by 40% in *db*/*db* mice. BVC suppressed serum levels of ALT and AST (Fig. 3c), which are commonly used to evaluate clinically hepatocellular injury, and it further ameliorated vacuolar degeneration in *db*/*db* livers (Fig. 3d). More significantly, similar results were observed in DIO mice (ESM Fig. 4). These findings indicated that BVC improves hepatotoxicity in *db*/*db* and DIO mice.

BVC regulates PPAR gene expression in vitro and in vivo To reveal the mechanism underlying BVC-mediated improvement in the metabolic syndrome, liver gene expression profiles of *db*/*db* and DIO mice were analysed by cDNA genome-wide gene expression assay. Figure 4a shows the 138 overlapping differential genes of both mouse livers that were identified (fold change ≥2, $p < 0.05$). Gene ontology pathway and hierarchical cluster analysis further revealed the most enriched pathways regulated by BVC were related to adipocytokine signalling, PPAR signalling, type 2 diabetes, glycerophospholipid metabolism, mitochondrial fatty acid beta oxidation and butanoate metabolism (Fig. 4b). Furthermore, the above results were confirmed by quantitative PCR. BVC increased the expression of the PPAR-γ marker gene glucose transporter 4 (*Glut4*, also known as *Slc2a4*) to enhance transport and utilisation of glucose in white adipose tissue (Fig. 4c) and skeletal muscle (Fig. 4d). BVC also upregulated other classic PPAR target

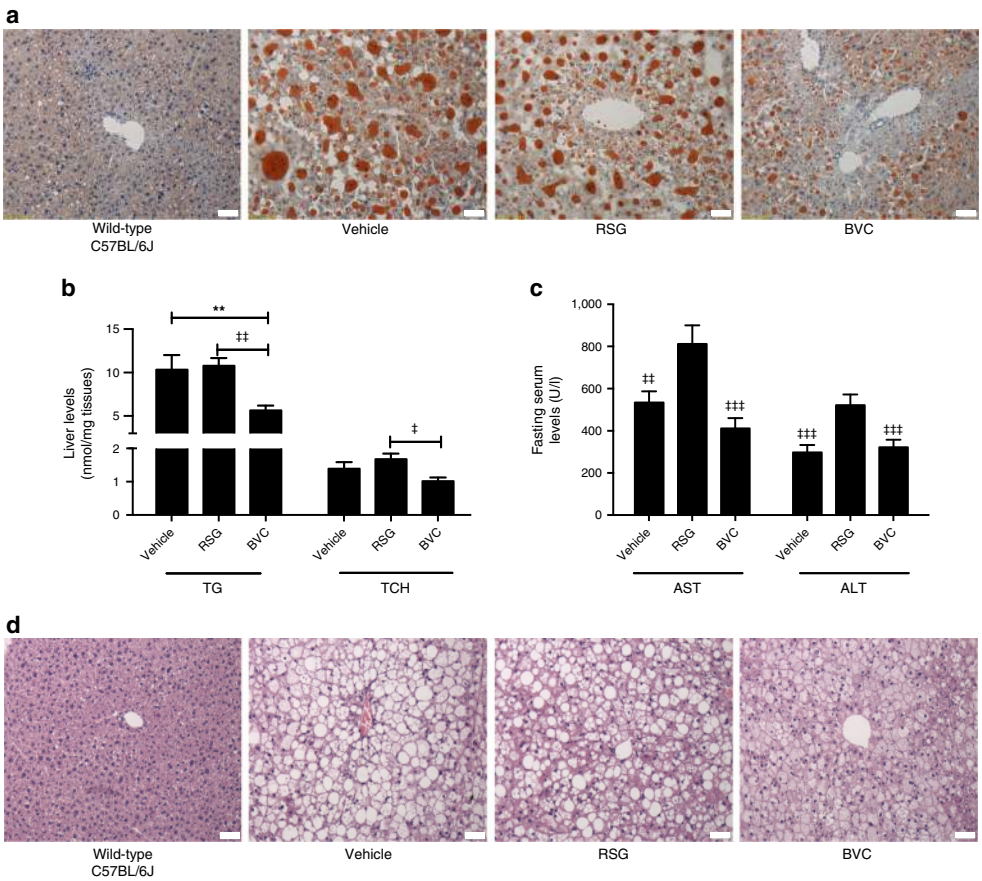

Fig. 3 BVC alleviated hepatotoxicity in *db*/*db* mice after 3 weeks of treatment. (**a**) Oil Red O staining of liver sections ($n = 9$), (**b**) liver TG and TCH contents ($n = 7$–9), (**c**) fasting serum AST and ALT levels ($n = 9$–10) and (**d**) H&E staining of liver sections ($n = 9$). $^{**}p < 0.01$ vs *db*/*db* mice exposed to vehicle. $^{‡}p < 0.05$, $^{‡‡}p < 0.01$ and $^{‡‡‡}p < 0.001$ vs RSG control. Scale bars, 50 μm

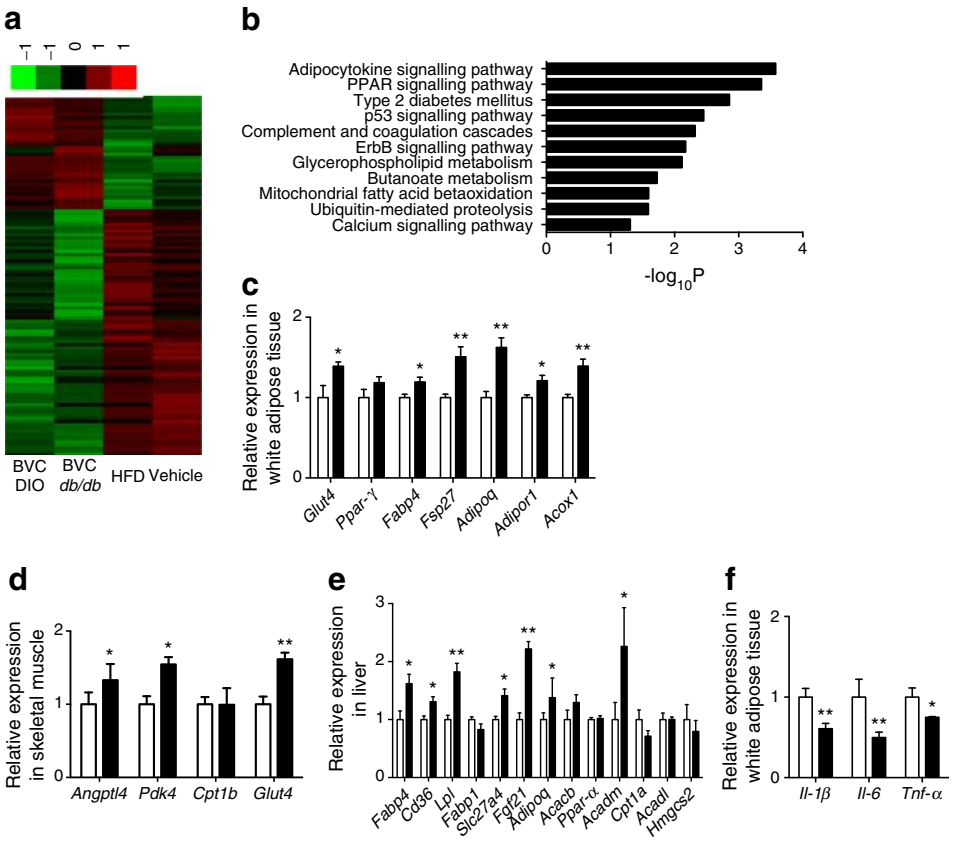

Fig. 4 BVC selectively regulates the expression of PPAR target genes. (**a**) Overlapped differential genes in livers of *db*/*db* and DIO mice with greater than twofold change ($n = 3$). (**b**) The 11 most enriched pathways ($p < 0.05$). (**c**–**e**) BVC regulated PPAR target genes in white adipose tissue (**c**), skeletal muscle (**d**) and liver (**e**) in *db*/*db* mice ($n = 6$). (**f**) BVC decreased the expression of inflammatory cytokines in white adipose tissue ($n = 6$). Data are expressed as mean ± SEM. *$p < 0.05$ and **$p < 0.01$ vs mice exposed to vehicle. *Ppar-γ* is also known as *Pparg*; *Ppar-α* is also known as *Ppara*

genes involved in the synthesis and transport of fatty acid and insulin sensitivity in white adipose tissue [31], such as *Fabp4*, *Acox1*, *Fsp27* (also known as as well as *Cidec*), *Adipoq* and *Adipor1* (Fig. 4c). Moreover, BVC significantly induced the expression of the PPAR-β/δ genes *Pdk4* and *Angptl4*, but not *Cpt1b*, in skeletal muscle (Fig. 4d). Additionally, BVC enhanced transport and β/ω-oxidation of fatty acid by inducing the expression of *Fabp4*, *Cd36, Lpl*, *Slc27a4*, *Fgf21*, *Acacb*, *Acadm* and *Acox1* but not *Cpt1a*, *Acadl* and *Hmgcs2* (Fig. 4e and ESM Fig. 5c). Finally, the expression of inflammatory cytokines *Tnf-α*, *Il-6* and *Il-1β* (also known as *Tnf*, *Il6* and *Il1b*) in white adipose tissue concurrent with insulin resistance was decreased by BVC (Fig. 4f). In contrast to RSG, BVC increased *Fgf21* mRNA expression to ameliorate insulin resistance and weight gain, but there was no difference in the expression of *Acacb*, *Acadm*, *Cpt1a*, *Acadl* and *Hmgcs2* in liver or *Cpt1b* in skeletal muscle (ESM Fig. 5a, b). In addition, BVC enhanced *Glut4* and *Cyp4a10* expression at day 2 and day 6, as well as the expression of *Cyp7a1* and *Scd1* at day 6 of exposure period of 3T3-L1 adipocyte differentiation, which is similar to RSG (ESM Fig. 5d–g). These data suggest that BVC enhances glucose transport and utilisation, hepatic lipid turnover and fatty acid metabolism through PPAR networks, thereby improving insulin sensitivity, dyslipidaemia and fatty liver [32].

BVC synergises with RSG and WY14643 in glucose-lowering effect Interestingly, in the reporter gene assay, BVC did not antagonise, but rather synergised with, synthetic PPAR-α and -γ agonists to induce PPAR-mediated transcription. In Fig. 5a, b, the combination of BVC plus RSG caused dose-dependent augmentation of the transactivation of LBDs and full-length PPAR-γ compared with 20 μmol/l RSG. Similar synergism was also observed when combining BVC with PGZ (ESM Fig. 6a, b). Consequently, the synergistic effects of BVC plus RSG on glucose metabolism were evaluated in *db*/*db* mice. With similar food intake (ESM Fig. 6c), the combination of 50 mg kg^{-1} day^{-1} BVC plus 2 mg kg^{-1} day^{-1} RSG significantly reduced body weight gain compared with 2 mg kg^{-1} day^{-1} RSG treatment ($p < 0.05$, ESM Fig. 6d). Compared with vehicle treatment, both BVC and RSG treatment significantly decreased fasting glucose concentrations in a dose-dependent manner (Fig. 5c). The combination of BVC plus RSG exhibited almost the same effects as 4 mg kg^{-1} day^{-1} RSG in lowering glucose levels, which was more effective than either treatment alone (Fig. 5c). Furthermore, BVC synergised with WY14643 (Fig. 5d, e) and fenofibric acid (ESM Fig. 6e, f) to induce the transcriptional activity of PPAR-α. However, no synergism between BVC with GW0742 in PPAR-β/δ-mediated transcription was detected (ESM Fig. 6g, h). Figure 5f showed that both BVC and fenofibrate dose-dependently decreased fasting TG levels

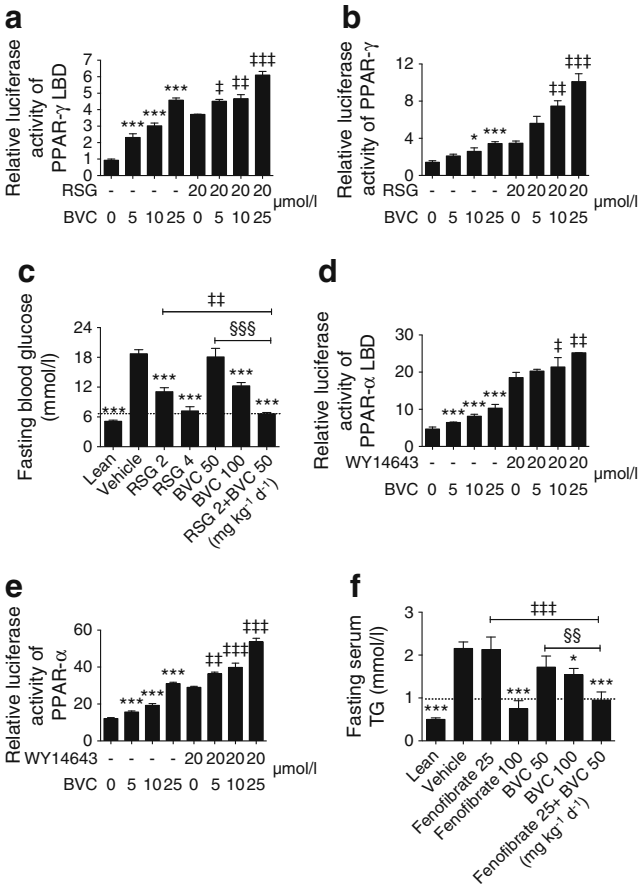

Fig. 5 BVC synergises with PPAR-γ and -α agonists in vitro and in vivo. (**a**, **b**) The combination of BVC plus RSG induced the transcriptional activities of mouse PPAR-γ ($n = 3$). (**c**) The effects on fasting blood glucose after 4 weeks of treatment ($n = 7$–11). (**d**, **e**) The effects of BVC plus fibrates on the transcriptional activities of mouse PPAR-α ($n = 3$) and (**f**) fasting TG levels ($n = 7$–11) of *db/db* mice. *$p < 0.05$ and ***$p < 0.001$ vs negative or vehicle control. ‡$p < 0.05$, ‡‡$p < 0.01$ and ‡‡‡$p < 0.001$ vs positive control. §§$p < 0.01$ and §§§$p < 0.001$ vs BVC 50 mg kg^{-1} day^{-1}. d, day

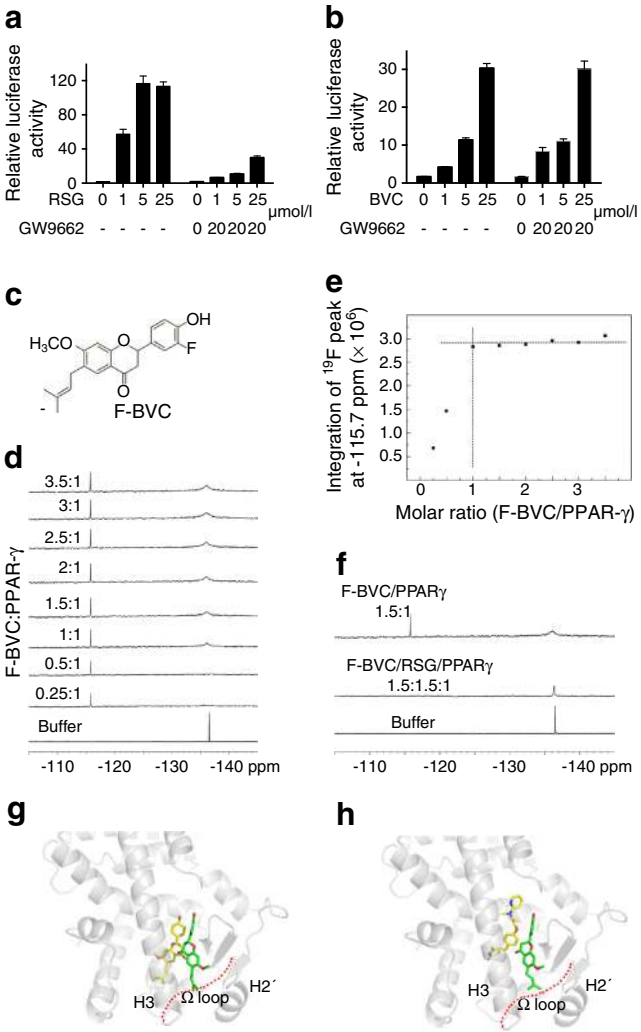

Fig. 6 Binding behaviour of BVC to PPAR-γ. (**a**, **b**) GW9662 blocked the transcriptional activities of PPAR-γ induced by RSG (**a**), but was not affected by BVC (**b**). Data are expressed as mean ± SEM. (**c**) The structure of F-BVC. (**d**) Titration of F-BVC resulted in two PPAR-γ LBD-bound ^{19}F-NMR resonances at −115.7 ppm and −136.1 ppm. (**e**) The ^{19}F-NMR resonance at −115.7 ppm was saturated at the ratio of 1:1 (ligand:PPAR-γ). (**f**) The disappearance of the ^{19}F chemical shifts at −115.7 ppm indicated that F-BVC shared the same canonical binding site as RSG on PPAR-γ. The retaining signal at −136.3 ppm suggested that F-BVC could occupy the other binding site after RSG bound to the CLBP of PPAR-γ. (**g**) Docking one BVC (yellow sticks) into the canonical site and the other BVC (green sticks) into the alternative site, respectively. (**h**) Docking of BVC (green sticks) into the alternative site after RSG (yellow sticks) occupies the CLBP. PPAR-γ is shown with the disordered Ω loop between H3 and H2′in red dashed lines

in *db*/*db* mice. Treatment with 50 mg kg^{-1} day^{-1} BVC plus 25 mg kg^{-1} day^{-1} fenofibrate treatment exhibited similar effects to 100 mg kg^{-1} day^{-1} fenofibrate treatment in lowering TG levels, which was more effective than either treatment alone ($p < 0.01$). The above results indicate BVC synergises with synthetic PPAR-γ and -α agonists in decreasing glucose and lipid levels.

Binding behaviour of BVC with PPAR-γ To study the binding events of BVC at the cellular level, the reporter gene assay was performed using a PPAR covalent antagonist GW9662, which can bind to the canonical ligand-binding pocket (CLBP) of synthetic PPAR ligands, blocking the binding to PPAR-LBD. Figure 6a, b as well as ESM Fig. 7a, b show that 20 μmol/l GW9662 reduced the transcriptional activities of PPAR induced by RSG and WY14643, but did not block the stimulation of BVC. The results demonstrate that BVC binds to at least one other binding site in PPAR in addition to the CLBP.

To further clarify the binding sites of BVC to PPAR-γ-LBD through ^{19}F-NMR, 3′-F-BVC (F-BVC; Fig. 6c) was prepared and validated as a potent PPAR activator (ESM Fig. 7c). Stoichiometric addition of F-BVC to PPAR-γ revealed sequential saturation of two binding sites as shown by ^{19}F chemical shifts at −115.7 ppm and −136.1 ppm (Fig. 6d). The ^{19}F-NMR

resonance at −115.7 ppm indicated F-BVC had a strong binding site in PPAR-γ, and it falls into a slow-exchange regime on the NMR time scale, resulting in the narrow line width of ^{19}F signal in bound form. Integration of ^{19}F-NMR signal at −115.7 ppm was plotted against titration molar ratio. As shown in Fig. 6e, the strong binding site was saturated at a ratio of 1:1 (ligand/PPAR-γ). In addition, the broader line width of the ^{19}F-NMR resonance at −136.1 ppm of F-BVC indicated the other weaker binding site in PPAR-γ, which may involve an intermediate chemical exchange between bound and free species of F-BVC. To further understand the binding behaviour of BVC, F-BVC was added into the sample of RSG-saturated PPAR-γ at the molar ratio of 1:1.5 (Fig. 6f). Compared with the ^{19}F resonance of F-BVC/PPAR-γ, the disappearance of the signal at −115.7 ppm indicated that F-BVC shared the same binding site (CLBP) in PPAR-γ as RSG, and RSG completely blocked BVC from binding to CLBP. Conversely, the retaining signal at −136.3 ppm confirmed that F-BVC occupied another site on PPAR-γ, but this binding could not be displaced by RSG.

Next, docking studies were performed to investigate the exact binding sites of BVC using the Glide program. Docking results further proved that BVC could bind to two binding sites in PPAR-γ. One is CLBP with the predicted docking score of −34.72 kJ/mol, and the other is a second binding site with a docking score of −28.03 kJ/mol, indicating BVC occupied the CLBP with higher binding affinity. The second binding site for BVC was consistent with the alternative binding site (ABS), which was composed of H2′, Ω loop, H3 and β sheets [33]. In addition, if one BVC was docked to CLBP first (Fig. 6g, yellow sticks), then a second BVC could be docked to the ABS with −25.94 kJ/mol (Fig. 6g, green sticks). If one RSG was docked to the CLBP first (Fig. 6h, yellow sticks), then BVC could bind to the ABS with −28.87 kJ/mol (Fig. 6h, green sticks). In addition, docking results showed that the 4′-hydroxy group formed a hydrogen bond with the guanidinium group of R288, and the 6-prenylated isoflavanone skeleton was surrounded by a hydrophobic subpocket composed of I281, F282, L353, L356, F360 and F363 (ESM Fig. 7d). In addition, the 7-methoxy group of BVC was surrounded by Y327, K367 and H449, where van der Waals forces play a dominant role in the interactions (ESM Fig. 7d). In conclusion, BVC could bind to CLBP and the alternative site in PPAR-γ, and RSG can block BVC binding to CLBP but not to the ABS.

Discussion

Matin et al have identified some synthetic flavanones, flavones and isoflavones as dual PPAR-α and -γ agonists [34], and further discovered some synthetic isoflavones that can activate three PPAR isoforms in vitro [35]. Here, for the first time, we identified BVC, a natural prenylated isoflavanone, as a potent pan-PPAR agonist. The prenylated group of flavones can produce an increased affinity for biological membranes and an improved interaction with proteins [36].

The in vitro functional analyses demonstrate that BVC binds to and activates three PPAR isoforms. Mouse studies conclude that BVC displays properties desired for a glucose-lowering pan-PPAR agonist. Previous studies have indicated that full agonism of PPAR-γ, as with RSG and PGZ, may be responsible for the side effects associated with glucose-lowering effects [37–39]. Therefore, BVC does not cause weight gain and hepatotoxicity because of its submaximal activation of PPAR-γ and additional activation of PPAR-α and -β/δ. The enhancement of fatty acid oxidation, with the decrease in uptake and synthesis of fatty acids and the associated increased lipid mobilisation in adipose tissue, hints at how PPAR-α activation leads to body weight gain and increased adiposity [40]. Activation of PPAR-β/δ has shown to increase the fatty-acid-burning capacity of skeletal muscle, which is accompanied by a redistribution of fatty acid flux adipose tissue toward skeletal muscle [41]. Thus, the sum of PPAR-α and PPAR-β/δ activation offsets fat accumulation and weight gain induced by PPAR-γ agonism. Also, the combination of PPAR-β/δ and PPAR-γ agonists has been shown to alleviate insulin resistance, regulate glucose metabolism and enhance the ability to exercise [11, 16, 42]. Therefore, BVC shows glucose-lowering effects without inducing weight gain and hepatotoxicity.

Interestingly, BVC synergises with synthetic PPAR-γ and -α agonists to improve carbohydrate and lipid metabolism, but not with PPAR-β/δ agonists. Reporter gene assays demonstrate that BVC synergises with synthetic agonists to induce transcriptional activities of PPAR-α and -γ. As a result, the synergistic effects are extensively confirmed in dose–response mouse studies. PPAR senses ligands through ligand-binding sites in the LBD [43, 44]. The PPAR-γ-LBD has shown two binding sites, CLBP and ABS; synthetic PPAR ligands are designed to bind to CLBP by mimicking endogenous ligands [33]. GW9662, a PPAR covalent antagonist, can compete for the CLBP of synthetic ligands to PPAR and block binding to CLBP. Reporter assays demonstrate that GW9662 blocks transcriptional activities of PPAR induced by RSG and WY14643, but does not antagonise BVC, which indicates that BVC has one additional binding site to the CLBP. Competitive binding and NMR studies demonstrate that BVC shares the CLBP with PPAR-α and -γ synthetic agonists. In addition, ^{19}F-NMR and docking results further reveal that BVC occupies the ABS in addition to the CLBP, although it binds to the CLBP with higher affinity than it binds to the ABS. After the CLBP of PPAR-γ is saturated with RSG, BVC continues to occupy the ABS. This unique binding mode of BVC produces special synergistic effects as a result of induced differential conformational change.

Although the LBDs of the three PPAR subtypes share 80% homology, the cavity of the PPAR-β/δ-LBD is markedly narrower than the LBDs of PPAR-α and -γ [45]. Thus, it is speculated that the PPAR-β/δ-LBD does not have enough room to accommodate two ligands, which could explain why BVC does not synergise with GW0742.

BVC binds to PPAR in a unique mode, resulting in a special conformational change, differential cofactor recruitment, gene expression and, finally, distinct biological responses. Agonist binding to PPAR-γ regulates activity by causing conformational changes to the transcription activation function-2 (AF-2) domain of the LBD [46]. Changes to AF-2 allow for coactivator recruitment, followed by transcriptional activation. These changes vary depending on the type of ligand that binds to the LBD. TZDs and fibrates induce direct stabilisation of AF-2 conformation through distinct interactions with helix 12 of the AF-2 domain, followed by the recruitment of coactivators, including PGC-1α and TRAP220 [33]. BVC does not recruit PGC-1α and TRAP220 during the transcriptional process—its unique binding mode results in indirect stabilisation of AF-2 mediated via an Ω loop and helix 3. Thus, BVC exhibits differential effects on the expression of PPAR target genes involved in fatty acid metabolism, cholesterol metabolism and glucose transport. As a result, BVC decreases TG and LDL-C levels in both mouse models, but RSG exhibits the discrepancies in lipid regulation, which are also probably linked to species-specific regulation of VLDL and LDL particle size and concentration, and apolipoprotein [47–49]. Compared with the only clinical pan-PPAR agonist bezafibrate, BVC exhibited a stronger glucose-lowering effect [17]. While another pan-PPAR agonist, LY465608, has been shown in preclinical studies to improve glucose and lipid disorders, it significantly increases body weight and causes severe hepatotoxicity [21, 23]. Although BVC exhibits broad-spectrum potency without inducing weight gain and hepatotoxicity, additional studies are required to assess the side-effect profiles of BVC compared with current PPAR agonists.

In conclusion, the synergistic effects occur because of the unique binding events of BVC to PPAR-α and -γ. Therefore, the combination of natural BVC plus TZDs or fibrates could help increase effectiveness with fewer doses, followed by controlled side effects. This discovery may provide a new promising therapeutic approach for the treatment of type 2 diabetes and other metabolic syndrome indications.

Acknowledgements The authors would like to thank W. Huang (Department of Diabetes and Metabolic Disease Research, Beckman Research Institute, City of Hope, Duarte, CA, USA) and Z. Yao (Department of Biochemistry, Microbiology & Immunology, Ottawa Institute of System Biology, University of Ottawa, Ottawa, ON, Canada) for their useful suggestions. We are grateful that B. Li (North American Biomedical Research Center, Los Angeles, CA, USA) revised the manuscript carefully.

Funding The studies were supported by the National Natural Science Fund (grant no. 81172951), Eastern Scholar Tracking Program of Shanghai Municipal Education Commission (2012-90), and 'Xinlin' Scholars and Shanghai E-Research Institute of Bioactive Constituent in TCM Plan.

Duality of interest The authors declare that there is no duality of interest associated with this manuscript.

Contribution statement LF designed the study, acquired and analysed data, drafted the manuscript and approved its final version. HL and KH acquired and analysed the NMR data, drafted the NMR part of manuscript and approved the final version. ZX, ZY and WZ analysed and interpreted docking data, drafted this part, and approved its final version. GD, YZ and LY acquired data, revised the manuscript's intellectual content and approved its final version. QT and KC contributed to the conception and design, revised the manuscript's intellectual content and approved its final version. FG, CH and YL contributed to the design and interpretation of data, revised the article for important intellectual content, and approved the final version. LF, CH and YL are responsible for the integrity of this work.

References

1. Cameron AJ, Shaw JE, Zimmet PZ (2004) The metabolic syndrome: prevalence in worldwide populations. Endocrinol Metab Clin N Am 33:351–375
2. Desvergne B, Wahli W (1999) Peroxisome proliferator-activated receptors: nuclear control of metabolism. Endocr Rev 20:649–688
3. Moraes LA, Piqueras L, Bishop-Bailey D (2006) Peroxisome proliferator-activated receptors and inflammation. Pharmacol Ther 110:371–385
4. Rubenstrunk A, Hanf R, Hum DW, Fruchart JC, Staels B (2007) Safety issues and prospects for future generations of PPAR modulators. Biochim Biophys Acta 1771:1065–1081
5. Lehmann JM, Moore LB, Smith-Oliver TA, Wilkison WO, Willson TM, Kliewer SA (1995) An antidiabetic thiazolidinedione is a high affinity ligand for peroxisome proliferator-activated receptor gamma (PPAR gamma). J Biol Chem 270:12953–12956
6. Schoonjans K, Auwerx J (2000) Thiazolidinediones: an update. Lancet 355:1008–1010
7. Olefsky JM (2000) Treatment of insulin resistance with peroxisome proliferator-activated receptor gamma agonists. J Clin Invest 106: 467–472
8. Ferre P (2004) The biology of peroxisome proliferator-activated receptors: relationship with lipid metabolism and insulin sensitivity. Diabetes 53(Suppl 1):S43–S50
9. Barish GD, Narkar VA, Evans RM (2006) PPAR delta: a dagger in the heart of the metabolic syndrome. J Clin Invest 116:590–597
10. Luquet S, Gaudel C, Holst D et al (2005) Roles of PPAR delta in lipid absorption and metabolism: a new target for the treatment of type 2 diabetes. Biochim Biophys Acta 1740:313–317
11. Brunmair B, Staniek K, Dorig J et al (2006) Activation of PPAR-delta in isolated rat skeletal muscle switches fuel preference from glucose to fatty acids. Diabetologia 49:2713–2722
12. Luquet S, Lopez-Soriano J, Holst D et al (2003) Peroxisome proliferator-activated receptor delta controls muscle development and oxidative capability. FASEB J 17:2299–2301
13. Wang YX, Zhang CL, Yu RT et al (2004) Regulation of muscle fiber type and running endurance by PPARδ. PLoS Biol 2:e294

14. Oliver WR Jr, Shenk JL, Snaith MR et al (2001) A selective peroxisome proliferator-activated receptor delta agonist promotes reverse cholesterol transport. Proc Natl Acad Sci U S A 98:5306–5311
15. Peters JM, Aoyama T, Burns AM, Gonzalez FJ (2003) Bezafibrate is a dual ligand for PPARalpha and PPARbeta: studies using null mice. Biochim Biophys Acta 1632:80–89
16. Tenenbaum A, Motro M, Fisman EZ (2005) Dual and pan-peroxisome proliferator-activated receptors (PPAR) co-agonism: the bezafibrate lessons. Cardiovasc Diabetol 4:14
17. Jones IR, Swai A, Taylor R, Miller M, Laker MF, Alberti KG (1990) Lowering of plasma glucose concentrations with bezafibrate in patients with moderately controlled NIDDM. Diabetes Care 13: 855–863
18. Chang F, Jaber LA, Berlie HD, O'Connell MB (2007) Evolution of peroxisome proliferator-activated receptor agonists. Ann Pharmacother 41:973–983
19. Singh MPPD, Sharma GK, Sharma CS (2011) Peroxisome proliferator-activated receptors (PPARs): a target with a broad therapeutic potential for human disease: an overview. Pharmacology 2: 58–89
20. Ramachandran U, Kumar R, Mittal A (2006) Fine tuning of PPAR ligands for type 2 diabetes and metabolic syndrome. Mini Rev Med Chem 6:563–573
21. Etgen GJ, Oldham BA, Johnson WT et al (2002) A tailored therapy for the metabolic syndrome: the dual peroxisome proliferator-activated receptor-alpha/gamma agonist LY465608 ameliorates insulin resistance and diabetic hyperglycemia while improving cardiovascular risk factors in preclinical models. Diabetes 51:1083–1087
22. Shearer BG, Billin AN (2007) The next generation of PPAR drugs: do we have the tools to find them? Biochim Biophys Acta 1771: 1082–1093
23. Guo Y, Jolly RA, Halstead BW et al (2007) Underlying mechanisms of pharmacology and toxicity of a novel PPAR agonist revealed using rodent and canine hepatocytes. Toxicol Sci 96:294–309
24. Mahindroo N, Huang CF, Peng YH et al (2005) Novel indole-based peroxisome proliferator-activated receptor agonists: design, SAR, structural biology, and biological activities. J Med Chem 48:8194–8208
25. Zining L (2013) Specification of syndrome differentiation on diabetic nephropathy. Guangzhou University of Chinese Medicine, Guangzhou, p28 (PhD thesis)
26. Chen Q, Zhu Y (2009) The effects of traditional Chinese medicine compound on diabetes. Chin J Med Guid 11:81–84
27. Zhang Y, Yu L, Cai W et al (2014) Protopanaxatriol, a novel PPARγ antagonist from *Panax ginseng*, alleviates steatosis in mice. Sci Rep 4:7375
28. Yamauchi T, Kamon J, Waki H et al (2001) The fat-derived hormone adiponectin reverses insulin resistance associated with both lipoatrophy and obesity. Nat Med 7:941–946
29. Brewer HB Jr (2004) Increasing HDL cholesterol levels. N Engl J Med 350:1491–1494
30. Marchesini G, Brizi M, Bianchi G et al (2001) Nonalcoholic fatty liver disease: a feature of the metabolic syndrome. Diabetes 50: 1844–1850
31. Monsalve FA, Pyarasani RD, Delgado-Lopez F, Moore-Carrasco R (2013) Peroxisome proliferator-activated receptor targets for the treatment of metabolic diseases. Mediat Inflamm 2013:549627
32. Ip E, Farrell GC, Robertson G, Hall P, Kirsch R, Leclercq I (2003) Central role of PPARalpha-dependent hepatic lipid turnover in dietary steatohepatitis in mice. Hepatology 38:123–132
33. Hughes TS, Giri PK, de Vera IM et al (2014) An alternate binding site for PPARγ ligands. Nat Commun 5:3571
34. Matin A, Gavande N, Kim MS et al (2009) 7-Hydroxy-benzopyran-4-one derivatives: a novel pharmacophore of peroxisome proliferator-activated receptor α and -γ (PPARα and γ) dual agonists. J Med Chem 52:6835–6850
35. Matin A, Doddareddy MR, Gavande N et al (2013) The discovery of novel isoflavone pan peroxisome proliferator-activated receptor agonists. Bioorg Med Chem 21:766–778
36. Botta B, Vitali A, Menendez P, Misiti D, Delle Monache G (2005) Prenylated flavonoids: pharmacology and biotechnology. Curr Med Chem 12:717–739
37. Weidner C, de Groot JC, Prasad A et al (2012) Amorfrutins are potent antidiabetic dietary natural products. Proc Natl Acad Sci U S A 109:7257–7262
38. Choi JH, Banks AS, Kamenecka TM et al (2011) Antidiabetic actions of a non-agonist PPARgamma ligand blocking Cdk5-mediated phosphorylation. Nature 477:477–481
39. Choi JH, Banks AS, Estall JL et al (2010) Anti-diabetic drugs inhibit obesity-linked phosphorylation of PPARγ by Cdk5. Nature 466:451–456
40. Ferreira AV, Parreira GG, Green A, Botion LM (2006) Effects of fenofibrate on lipid metabolism in adipose tissue of rats. Metab Clin Exp 55:731–735
41. Fredenrich A, Grimaldi PA (2005) PPAR delta: an uncompletely known nuclear receptor. Diabetes Metab 31:23–27
42. Balakumar P, Rose M, Ganti SS, Krishan P, Singh M (2007) PPAR dual agonists: are they opening Pandora's Box? Pharmacol Res 56: 91–98
43. Kliewer SA, Umesono K, Noonan DJ, Heyman RA, Evans RM (1992) Convergence of 9-cis retinoic acid and peroxisome proliferator signalling pathways through heterodimer formation of their receptors. Nature 358:771–774
44. Berger J, Moller DE (2002) The mechanisms of action of PPARs. Annu Rev Med 53:409–435
45. Zoete V, Grosdidier A, Michielin O (2007) Peroxisome proliferator-activated receptor structures: ligand specificity, molecular switch and interactions with regulators. Biochim Biophys Acta 1771: 915–925
46. Kallenberger BC, Love JD, Chatterjee VK, Schwabe JW (2003) A dynamic mechanism of nuclear receptor activation and its perturbation in a human disease. Nat Struct Biol 10:136–140
47. Fernandes-Santos C, Carneiro RE, de Souza Mendonca L, Aguila MB, Mandarim-de-Lacerda CA (2009) Pan-PPAR agonist beneficial effects in overweight mice fed a high-fat high-sucrose diet. Nutrition 25:818–827
48. Goldberg RB, Kendall DM, Deeg MA et al (2005) A comparison of lipid and glycemic effects of pioglitazone and rosiglitazone in patients with type 2 diabetes and dyslipidemia. Diabetes Care 28: 1547–1554
49. Deeg MA, Buse JB, Goldberg RB et al (2007) Pioglitazone and rosiglitazone have different effects on serum lipoprotein particle concentrations and sizes in patients with type 2 diabetes and dyslipidemia. Diabetes Care 30:2458–2464